Pharm Res (2014) 31:1015–1031
DOI 10.1007/s11095-013-1224-z

RESEARCH PAPER

Comparison of PLA Microparticles and Alum as Adjuvants for H5N1 Influenza Split Vaccine: Adjuvanticity Evaluation and Preliminary Action Mode Analysis

Weifeng Zhang • Lianyan Wang • Yuan Liu • Xiaoming Chen • Jiahui Li • Tingyuan Yang • Wenqi An • Xiaowei Ma • Ruowen Pan • Guanghui Ma

Received: 17 June 2013 / Accepted: 3 October 2013 / Published online: 30 October 2013

ABSTRACT

Purpose To compare the adjuvanticity of polymeric particles (new-generation adjuvant) and alum (the traditional and FDA-approved adjuvant) for H5N1 influenza split vaccine, and to investigate respective action mode.

Methods Vaccine formulations were prepared by incubating lyophilized poly(lactic acid) (PLA) microparticles or alum within antigen solution. Antigen-specific immune responses in mice were evaluated using ELISA, ELISpot, and flow cytometry assay. Adjuvants' action modes were investigated by determining antigen persistence at injection sites, local inflammation response, antigen transport into draining lymph node, and activation of DCs in secondary lymphoid organs (SLOs).

Results Alum promoted antigen-specific humoral immune response. PLA microparticles augmented both humoral immune response and cell-mediated-immunity which might enhance cross-protection of influenza vaccine. With regard to action mode, alum adjuvant functions by improving antigen persistence at injection sites, inducing severe local inflammation, slightly improving antigen transport into draining lymph nodes, and improving the expression of MHC II on DCs in SLOs. PLA microparticles function by slightly improving antigen transport into draining lymph nodes, and promoting the expression of both MHC molecules and co-stimulatory molecules on DCs in SLOs.

Conclusions Considering the adjuvanticity and side effects (local inflammation) of both adjuvants, we conclude that PLA microparticles are promising alternative adjuvant for H5N1 influenza split vaccine.

KEY WORDS adjuvanticity · alum · influenza vaccine · microparticles · mode of action

ABBREVIATIONS

Ag	Antigen
Alum	Aluminum hydroxide
APC	Antigen presenting cell
BSA	Bovine serum albumin
DCs	Dendritic cells
ELISA	Enzyme-linked immunosorbant assay
ELISpot	Enzyme-linked immunospot
HA	Hemagglutination
HI	Hemagglutination inhibition
MHC	Major histocompatibility complex
O/W	Oil in water
PLA	Poly(lactic acid)
SEM	Standard errors of mean
SLOs	Secondary lymphoid organs
TMB	3,3′,5,5′-tetramethylbenzidine

Weifeng Zhang and Lianyan Wang has contributed equally.

Electronic supplementary material The online version of this article (doi:10.1007/s11095-013-1224-z) contains supplementary material, which is available to authorized users.

W. Zhang • L. Wang • Y. Liu • X. Chen • J. Li • T. Yang • G. Ma (✉)
National Key Laboratory of Biochemical Engineering
PLA Key Laboratory of Biopharmaceutical Production & Formulation Engineering, Institute of Process Engineering
Chinese Academy of Sciences, Bei-Er-Jie No.1, Zhong-Guan-Cun
Haidian District Beijing 100190, People's Republic of China
e-mail: ghma@home.ipe.ac.cn

W. Zhang • Y. Liu • X. Chen
University of Chinese Academy of Sciences, Beijing 100049
People's Republic of China

W. An • X. Ma • R. Pan
Hualan Biological Engineering, Inc., Xinxiang 453003, Henan Province
People's Republic of China

INTRODUCTION

Influenza, often causing worldwide seasonal epidemics or even pandemics, is a significant cause of morbidity and mortality (1). H5N1 influenza is a highly pathogenic avian influenza strain, and usually causes high morbidity and high mortality. Frequent outbreaks in recent years and the increasing number of human infections have accentuated the urgency to develop safe and effective vaccines to prevent a potential H5N1 influenza pandemic (2). Vaccines prepared from attenuated or inactivated viruses have been successfully used to deal with influenza viruses in some degree. However, the side effects and potential safety concerns restrict their application. Subunit vaccines, such as split vaccine or subvirion vaccine, are regarded as safer alternatives to vaccines based on attenuated or inactivated viruses, because they lack the molecular machinery to cause an infection or to induce severe inflammation.

The inadequacy of subunit vaccines is low immunogenicity, owing to the absence of the inherent immunostimulatory ability of viruses (3). Thus, adjuvants must be employed to augment the immune response to subunit vaccines. Another challenge for influenza vaccine development is the high variability of influenza viruses due to antigenic drift or/and antigenic shift. Because of the frequent mutations, influenza vaccines must be re-developed and updated every year. Therefore, a major goal in influenza vaccine development is to induce broad immunological cross-protection. Consequently, adjuvants, when used with influenza vaccines, should enhance both humoral and cellular immune responses, because the cross-protection ability of influenza vaccines is primarily attributed to the cell-mediated immunity especially the $CD8^+$ cytotoxic T lymphocytes (CTL)-mediated immune response (1,2,4–8).

Alum is a conventional adjuvant that has been used for over 80 years, and is the only adjuvant widely licensed for human use (9). As an adjuvant, alum augments the potency and efficacy of immune response to co-administrated antigen, and has been used in numerous licenced vaccines, including vaccines for hepatitis A virus, hepatitis B virus, human papillomavirus, diphtheria and tetanus (DT), haemophilus influenza type B, and pneumococcal conjugate vaccines (10,11). With the development of vaccinology, new generation of adjuvants were extensively investigated to meet the needs of novel vaccines. Among them, particulate-based delivery system is a competitive one. Particulate-based adjuvants employ the use of particulates with dimensions comparable to those of pathogens with which the immune system has evolved to combat. Recent studies have demonstrated that particulate-based adjuvants can promote vaccine-elicited immune responses by increasing antigen persistence at injection sites, improving the access of antigen to antigen presenting cells (APCs), activating NALP3 inflammasome of APCs, and adjusting the pathway of antigen presentation (12–15). In the past decades, biodegradable polymeric micro/nano-particles have extensively aroused researchers' concerns, because they commendably accord with the prerequisites of an "ideal adjuvant": eliciting a persistent, high quality immune response to antigen, biodegradable, non-toxic, non-immunogenic, and chemically defined for reproducible manufacture (16). In addition, approval by FDA and ease to be processed into micro/nano-particles make poly(lactic acid) (PLA) become one of the most popular materials for micro/nano-particles fabrication.

Although alum and PLA-based particles as adjuvants for various vaccines, including influenza vaccine, have been reported, it is still unclear which one (alum or PLA-based particles) is better adjuvant for H5N1 influenza split vaccine. To clarify this uncertainity, this study aim to compare the adjuvanticity of PLA microparticles and alum for H5N1 influenza split vaccine, and to illuminate respective mode of action. We prepared PLA microparticles with narrow size distribution by a facile method combining O/W emulsion-solvent evaporation method and premix membrane emulsification technique (17). Vaccine formulations were prepared by adsorption-mixture combined method, *i.e.* simply incubating PLA microparticles (or alum) within the solution of split vaccine. Antigen-specific antibodies response (IgM, IgG, IgG1, IgG2a, and IgG2b) in sera collected from vaccinated mice were detected by enzyme-linked immunosorbent assay (ELISA) and hemagglutination inhibition assay. Lymphocytes activation, T cells responses, and maturation and activation of DCs in secondary lymphoid organs were evaluated by flow cytometry. *In vivo* imaging and histochemistry assay were performed to assess antigen persistence at injection site and local inflammation, respectively.

MATERIALS AND METHODS

Mice and Reagents

Balb/c mice (female, 4–6 weeks old) were provided by Vital River Laboratories (Beijing, China). All animal studies were performed in accordance with Guide for the Care and Use of Laboratory Animals, and approved by Experimental Animal Ethics Committee in Beijing. Influenza virus split vaccine (A/Anhui/1/2005(H5N1)) and alum adjuvant ($Al(OH)_3$) were kindly provided by Hualan Vaccine Inc. (Henan, China). Poly(D,L-lactic acid) (PLA, Mw≈10 kDa) was purchased from the Institute of Medical Instrument (Shandong, China). Poly(vinyl alcohol) (PVA-217, degree of polymerization 1700, degree of hydrolysis 88.5%) was kindly provided by Kuraray (Tokyo, Japan). Premix membrane emulsification equipment (FMEM-500M) was provided by the National Engineering Research Center for Biotechnology (Beijing, China). Shirasu porous glass (SPG) membrane was provided by SPG Technology Co. Ltd. (Sadowara, Japan). The medium for splenocytes culture was RPMI 1640 (Gibco, Carlsbad, CA, USA) with 10% (v/v) fetal bovine serum (Gibco, Carlsbad, CA, USA). All fluorescence-labelled anti-mouse antibodies were purchased from eBioscience (CA, USA).

ELISpot^{PLUS} kits were obtained from Mabtech AB (Nacka Strand, Sweden). All other reagents were of analytical grade.

Preparation and Characterization of PLA Microparticles

PLA microparticles were prepared by oil-in-water emulsion-solvent evaporation method combined with SPG membrane emulsification technique (17). Briefly, 200 mg PLA in 5 ml methylene chloride was emulsified in 50 ml PVA solution (1.9%, m/v) to form coarse emulsion. Then, this coarse emulsion was extruded through the SPG membrane (pore size, 2.8 μm) under a certain nitrogen pressure for 5 times and uniform-sized emulsions were obtained. The emulsions droplets were solidified into microparticles by stirring overnight to evaporate the organic solvent methylene chloride. PLA microparticles were then collected by centrifugation (5,000 rpm, 5 min), and further washed with deionized water 5 times to remove the residual PVA. Finally, PLA microparticles were freeze-dried and stored at room temperature.

The size and zeta potential of PLA microparticles were measured using ZetaPlus apparatus (Brookhaven Instrument, Holtsville, NY, USA). The morphology of PLA microparticles was characterized by scanning electron microscopy (JEM-6700F, JEOL Ltd., Tokyo, Japan).

Preparation and Characterization of Vaccine Formulations with Different Adjuvants

PLA microparticles (or alum)-adjuvanted vaccine formulation was prepared by incubating 5.0 mg lyophilized microparticles (or 0.9 mg $Al(OH)_3$) within 1.0 ml solution of split vaccine (Hemagglutinin (HA) concentration, 20 μg/ml in 10 μM PBS containing 0.85% (m/v) NaCl, pH 7.2) overnight at 25°C in a vertical mixer. The mixture without removing unbound antigen was conserved at 4°C for subsequent animals immunization.

To further confirm the adsorption of antigen on microparticles, antigen was labelled with fluorophore Cy5. Microparticles with Cy5-labelled antigen adsorbed were observed by TCS SP5 Confocal Laser Scanning Microscopy (Leica, Solms, Germany). The fluorescence distribution profiles across each microparticle were analyzed by LeicaLASAF software. Micro Bicinchoninic acid (BCA) Protein Assay Reagent Kit (Pierce, Rockford, USA) was utilized to measure the antigen adsorption efficiency (AE). The mixture was centrifuged at 6, 000 rpm for 5 min and antigen concentration in the supernatant was detected according to manufacturer's instructions. The AE was calculated using the following formula:

$$\mathrm{AE}(\%) = \frac{\text{antigen content in mixture} - \text{antigen content in supernatant}}{\text{antigen content in mixture}} \times 100\%.$$

Animal Immunization

Female Balb/c mice (4–6 weeks old, $n = 6$) were immunized with either split vaccine alone, alum-adjuvanted vaccine, or PLA microparticles-adjuvanted vaccine, by intramuscular injection in the hind legs twice at a 2-week interval. The dose of HA was 3 μg in 150 μl buffer per mouse for each immunization (half dose for one injection site, *i.e.* each hind leg). Serum was collected from retro orbital plexus of the mice at designated time points (*i.e.* 7, 14, 21, and 28 days post primary immunization). On day 28 post primary immunization, splenocytes were harvested for ELISpot and flow cytometry assay.

Determination of IgM, IgG, IgG1, IgG2a, and IgG2b

Antigen-specific IgM, IgG, IgG1, IgG2a, and IgG2b in serum were quantitatively determined by ELISA as previously described (18,19). Briefly, 96-wells ELISA plates (Costar, New York, USA) were coated with 200 ng of influenza split vaccine antigen (H5N1) per well in coating buffer (0.05 M CBS, pH 9.6). Plates were washed with PBST (0.01 M PBS containing 0.05% (m/v) Tween 20, pH 7.4) and blocked by incubating with 2% (m/v) BSA in PBST for 60 min at 37°C. Subsequently, the plates were washed with PBST for 3 times. Appropriate dilutions of sera were applied to the plates, serially diluted twofold in diluting buffer (PBST containing 0.1% (m/v) BSA), and incubated for 30 min at 37°C. Plates were then washed and incubated with horseradish peroxidase-conjugated goat antibodies against mouse IgM (SouthernBiotech, 1:6000), IgG (Sigma, 1:20000), IgG1, IgG2a, or IgG2b (Santa cruz, 1:2000) for 30 min at 37°C. Thereafter, the plates were washed with PBST and incubated with 3,3′,5,5′-tetramethylbenzidine (TMB) substrate (Sigma) for 20 min at room temperature in dark. After terminated by adding 50 μl 2 M H_2SO_4 per well, the optical density (OD, 450 nm) was measured by Infinite M200 Microplate Spectrophotometer (Tecan, Männedorf, Switzerland). Titers were given as the reciprocal sample dilution corresponding to, twice higher of OD than that of negative sera (IgG, IgG1, IgG2a, and IgG2b), or OD above 0.35 (IgM).

Hemagglutination Inhibition (HI) Assay

The HI assay was carried out as previously described (18,20). First, 6 μl of serum collected at 28 days post primary immunization was incubated overnight at 37°C with 24 μl Receptor Destroying Enzyme (RDE) solution to suppress nonspecific hemagglutination inhibition. The mixture was then incubated at 56°C for 30 min to inactivate RDE. Next, 90 μl PBS was added to obtain a final 20-fold serum dilution. 50 μl diluted serum was transferred in duplicate to V-bottom 96-wells

plates (Xinkang, Jiangyan/Jiangsu, China) and serially diluted two-fold in PBS. Next, four hemagglutination units (HAU) Influenza A/Anhui/1/2005 (H5N1) split vaccine in 25 μl PBS was added into all wells and the mixture was incubated for 30 min at room temperature. Finally, 25 μl 1% (v/v) chicken erythrocytes in PBS were added into all wells and the plates were incubated for 40 min at room temperature. The HI titer was expressed as the reciprocal value of the highest serum dilution which could complete inhibit the hemagglutination of chicken erythrocytes.

Determination of Th1 Cytokines by Enzyme-Linked Immunospot (ELISpot) Assay

The splenocytes harvested from the vaccinated mice at 28 days post primary immunization were measured for IFN-γ, IL-2, and IL-12 by ELISpot^{PLUS} kits (Mabtech AB, Nacka Strand, Sweden). According to the manufacturer's instructions, the ELISpot plates were activated with ethanol and then incubated with coating antibodies overnight at 4°C. Then, 1.0×10^5 splenocytes in 100 μl medium with H5N1 influenza split vaccine (0.25 μg HA) as stimulatory agent were added into the wells and the plates were incubated for 36 h in a 37°C humidified incubator with 5% CO_2. After emptying and washing the plates, the detection antibodies were added and the plates were incubated for 2 h at room temperature, followed by adding Streptavidin-ALP and incubating for 1 h at room temperature. Finally, the ready-to-use substrate solution (BCIP/NBT-plus) was added to the plates and colour development was stopped by washing extensively in tap water after distinct spots emerging. The spots were inspected and counted in an ELISpot analysis system (SageCreation, Beijing, China).

Determination of Cytokines and Granzyme B by ELISA

Balb/c mice ($n=6$) were intramuscularly vaccinated twice at a 2-week interval. On day 28 post primary immunization, mice were euthanized, and splenocytes were harvested and stimulated with HA (HA, 2.0 μg/ml; splenocytes, 4.0×10^6 cells/ml) for 48 h in a 37°C humidified incubator with 5% CO_2. The supernatant was collected by centrifugation (500×g, 5 min). The concentration of cytokines (IFN-γ and IL-4) and granzyme B in the supernatant was measured by ELISA kits (eBioscience, CA, USA), according to the manufacturer's instructions.

Evaluation of Lymphocytes Activation and T Cell Response by Flow Cytometry Assay

Flow cytometry assay was conducted to evaluate the effect of PLA microparticles and alum on lymphocytes activation, effector/effector memory T cell response, and antigen-specific $CD8^+$ T cell response. Balb/c mice ($n=6$) were intramuscularly vaccinated twice at a 2-week interval. On day 28 post primary immunization, mice were euthanized, and splenocytes were harvested and stimulated with HA (HA, 2.5 μg/ml; splenocytes, 5.0×10^6 cells/ml) for 72 h in a 37°C humidified incubator with 5% CO_2. After washed, cells were stained with fluorescence-labelled anti-mouse antibodies against CD4, CD8, CD19, CD69, CD44, CD62L (eBioscience, CA, USA) and peptide-MHC pentamers (APC-labelled IYSTVASSL/H-2Kd pentamer, Proimmune, FL, USA). CyAn™ ADP flow cytometer (Beckman Coulter, California, USA) was utilized to determine the percentages of activated lymphocytes ($CD69^+$), effector memory T cells ($CD44^{hi}CD62L^{low}$), and antigen-specific $CD8^+$ T cells ($CD8^+$IYSTVASSL-MHC I^+). Data analysis was performed using Summit software (version 4.3).

Antigen Persistence at Injection Sites

To monitor antigen persistence at injection sites *in vivo*, antigen was labeled with a near infrared dye Cy7 mono-reactive NHS ester (Fanbo Biochemicals, Beijing, China). Balb/c mice ($n=6$) were intramuscularly injected with different vaccine formulations containing Cy7-labelled antigen (3 μg HA in 150 μl buffer for one mouse, half dose at each site). The retention of antigen at injection sites was documented by Carestream FX PRO *in vivo* imaging system at the indicated time points (ex: 730 nm; em: 790 nm). Carestream Molecular Imaging Software was used to quantify sum fluorescence intensity at the injection sites.

Determination of Local Inflammation by Histochemical Evaluation

Vaccine-associated inflammation at injection sites was evaluated by histological analysis. Balb/c mice ($n=3$) were intramuscularly injected with different vaccine formulations (antigen containing 3 μg HA in 150 μl buffer, half dose at one site). At the time points of 2 days and 7 days post injection, muscles at injection sites were isolated from mice, embedded into paraffin, sectioned, and stained with hematoxylin and eosin. Histological micrographs were captured using Olympus BX51 microscope.

Expression of MHC Molecules and Co-stimulatory Molecules on Dendritic Cells in Secondary Lymphoid Organs

Balb/c mice ($n=3$) were intramuscularly vaccinated with different vaccine formulations (antigen containing 3 μg HA in 150 μl buffer, half dose at one site). At the indicated time points post immunization, mice were euthanized. Sciatic lymph nodes, popliteal lymph nodes, and spleen were

harvested and processed into single cell suspension. Cells were stained with fluorescence-labelled anti-mouse antibodies against CD11c, MHC I, MHC II, CD86 (eBioscience), and CD80 (BioLegend). CD11c, the common marker of DCs subsets in lymph nodes and spleen, was used to indetify DCs. Expression of MHC molecules and co-stimulatory molecules on dendritic cells was determined by CyAn™ ADP flow cytometer (Beckman Coulter, California, USA) and analyzed using Summit software (version 4.3.02).

Statistical Analysis

Statistical analysis was performed using GraphPad Prism 5.0 software (San Diego, CA, USA). All data in this study were shown as mean ± standard error of the mean (SEM). Differences between two groups were tested by unpaired, two-tailed Student's *t* test. Differences among multiple groups were tested by one-way ANOVA followed by Tukey's multiple comparison. Significant differences between the groups were expressed as follows: $*p<0.05$, $**p<0.01$, and $***p<0.001$.

RESULTS

Characteristics of PLA Microparticles and Vaccine Formulations with Different Adjuvants

PLA microparticles were prepared by an O/W emulsion-solvent evaporation method combined with premix membrane emulsification technique (Fig. 1a). Scanning electron micrograph revealed that PLA microparticles exhibited the desired spherical shapes (Fig. 1b). In addition, the size distribution (Fig. 1c) showed that the mean particle diameter was about 820 nm with a narrow size distribution. The zeta potential of PLA microparticles was about −17.05 mV, indicating negative surface charge.

The vaccine formulations with different adjuvants were prepared by incubating antigen solution with adjuvants (alum and PLA microparticles). Confocal laser scanning microscopy was utilized to characterize the adsorption of antigen on microparticles. Results showed that antigen adsorbed on PLA microparticles (Fig. 1d), and the fluorescence distribution profile of individual particles indicated that antigen mainly adsorbed on the surface of particles (Fig. 1e). We characterized the size, zeta potential, and morphology of PLA microparticles both before/after freeze-drying and before/after adsorption. We found that lyophilization and antigen adsorption had little effect on the size, zeta potential, and morphology of PLA microparticles (data not shown).

Antigen concentrations before and after antigen adsorption were measured by Micro BCA kit, and antigen adsorption efficiency (AE) was calculated. Antigen AE of alum was above 85%, while antigen AE of PLA microparticles was very low (about 5%). The isoelectric point of antigen was 5.4, and therefore antigen was negatively charged in adsorbing buffer (pH 7.2). The powerful adsorption ability of alum was based on the strong electrostatic interaction between positively charged alum (aluminium hydroxide) and negatively charged antigen (9). The adsorption of antigen onto polymeric microparticles were drived by multiple driving forces, including electrostatic interaction, van der Waals force, hydrophobic interaction, and so on (21). The repulsive force between negatively charged PLA microparticles and negatively charged antigen depressed the antigen adsorption, resulting in the low antigen adsorption efficiency.

PLA Microparticles-Adjuvanted Vaccine Elicited Superior Antibody Response and Th1-Polarization to Alum-Based Vaccine

Having confirmed antigen adsorption, we next wanted to determine the efficacy of each adjuvant. To begin, we measured antigen-specific IgM, IgG, IgG1, IgG2a, and IgG2b titers in immunized mice.

On day 7 post primary immunization, PLA microparticles-adjuvanted vaccine induced significantly higher IgM titer than alum-adjuvanted vaccine and split vaccine alone (Fig. 2a). The strong IgM response indicated a more effective protection against pathogens in the early stage after vaccination. Both adjuvants didn't dramatically improve IgG production on day 7 post primary vaccination. However, at 14, 21, and 28 days after primary immunization, mice immunized with PLA microparticles-adjuvanted vaccine developed strong IgG responses, comparable to that induced by alum-adjuvanted vaccine, and significantly stronger (2.8–14.2 fold) than that induced by soluble antigen (Fig. 2b).

To investigate the effect of both adjuvants on Th1/Th2 polarization of the immune response, the IgG subclass profiles (on day 28 post primary immunization) elicited by these different vaccine formulations were determined. As shown in Fig. 2c, PLA microparticles-adjuvanted vaccine and alum-adjuvanted vaccine induced comparable levels of IgG1 and IgG2a titers which were remarkably higher than that for soluble antigen. However, the IgG2b titer for alum-adjuvanted vaccine was similar to that for split vaccine alone, and dramatically lower than that for PLA microparticles-adjuvanted vaccine. In addition, ratios of IgG2a/IgG1 and IgG2b/IgG1 for PLA microparticles-adjuvanted vaccine were significantly higher than those for alum-adjuvanted vaccine (Fig. 2d). These data suggested that PLA microparticles could induce stronger Th1-associated immunity than alum.

Haemagglutinin (HA), the main glycoprotein on the surface of influenza virus, plays an important role in binding to cell-surface receptors and facilitating viral envelope-endosomal membrane fusion, and is the main target antigen

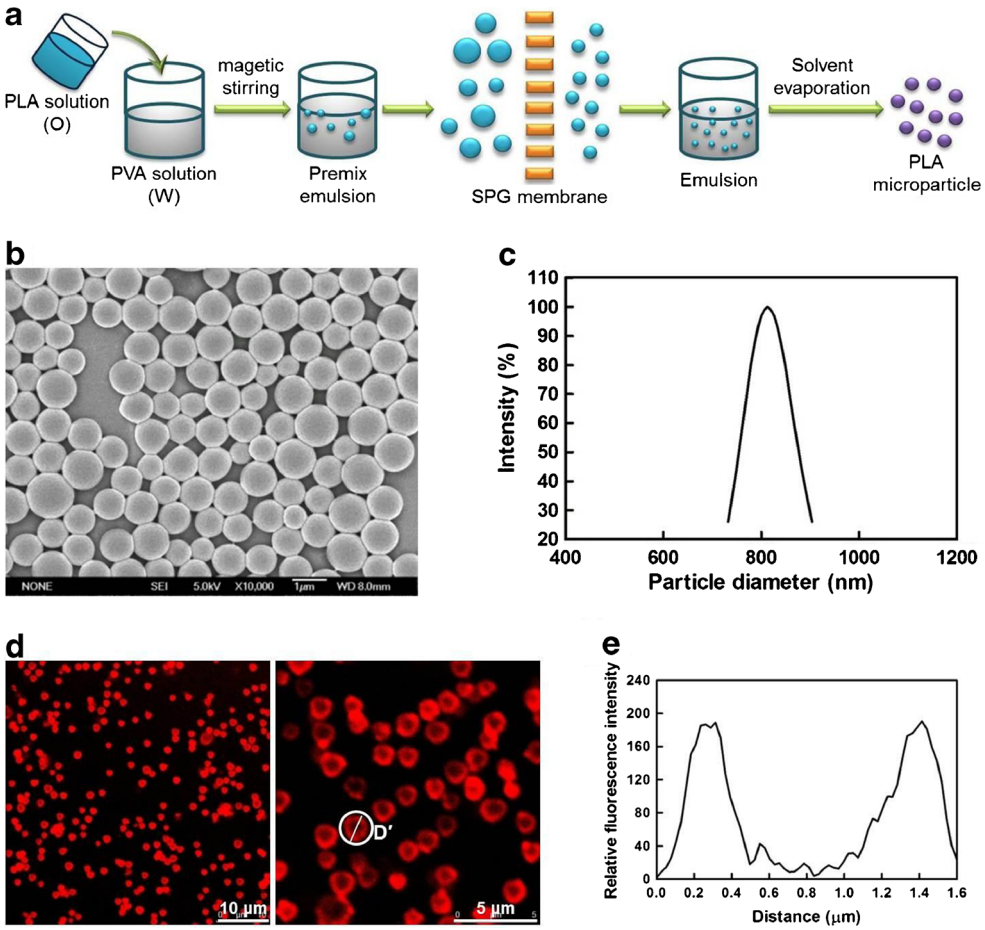

Fig. 1 Preparation and characterization of PLA microparticles and PLA microparticles-adjuvanted vaccine formulation. (**a**) Schematic illustration of PLA microparticles preparation by O/W emulsion-solvent evaporation method combined with premix membrane emulsification technique. (**b**) Scanning electron micrograph and (**c**) size distribution profile of PLA microparticles. (**d**) Confocal laser scanning micrographs of PLA microparticles with Cy5-labelled antigen adsorbed. (**e**) The profile of fluorescence intensity across one Cy5-labelled antigen adsorbed microparticle (D′). The scale bar in (**b**) represents 1 μm.

of humoral responses (22). Therefore, HI assay was performed to evaluate anti-HA antibody levels (on day 28 post primary immunization) in vaccinated mice. As shown in Fig. 2e, compared to soluble antigen, significantly higher HI titers were achieved by both adjuvanted vaccines. However, HI titer elicited by PLA microparticles-adjuvanted vaccine was significantly higher than that by alum-based vaccine.

PLA Microparticles Exerted Stronger Adjuvanticity than Alum for Th1-Polarization, Lymphocytes Activation, and T Cell Response

To further explore the adjuvanticity of PLA microparticles and alum, we next evaluated cytokines secretion, lymphocytes activation, effector memory T cell response, and antigen-specific $CD8^+$ T cell response in splenocytes restimulated *in vitro*.

ELISpot assay was performed to detect secretion of Th1 cytokines (indicators for Th1-type immune response) by splenocytes. Compared to soluble antigen, employment of PLA microparticles remarkably improved the secretion of IFN-γ, IL-2, and IL-12 by splenocytes (Fig. 3a–c). However, alum adjuvant didn't augment the secretion of these Th1 cytokines, and even dramatically reduced the secretion of IFN-γ which played an important role in improving differentiation of $CD4^+$ Th0 cells to $CD4^+$ Th1 cells, predominantly directing IgG2a isotype switching (23), and promoting cytotoxic T cell response (Fig. 3a). Th1 cytokines could directly promote cell-mediated-immunity (23). IL-2 is produced by $CD4^+$ Th1 cells and $CD8^+$ T cells, and plays an important role in antigen-specific proliferation of helper and cytotoxic T cells. IL-12, produced mainly by macrophages and DCs, aids to Th1 skewing of immune response. To further analyze the Th1/Th2 balance of immune response, we determined the secretion of both Th1 cytokine (IFN-γ) and Th2 cytokine (IL-4) by splenocytes. Compared to alum, PLA microparticles-adjuvanted vaccine induced significantly higher secretion levels of both IFN-γ (Fig. 3d) and IL-4 (Fig. 3e). As shown in Fig. 3f, the IFN-γ:IL-4 ratio for PLA microparticles was significantly higher than that for alum vaccine. Thus, these data indicated that PLA microparticles exerted stronger adjuvanticity than alum for Th1-polarization of vaccine-induced immune response.

CD69 has been recognized as an early marker of activated lymphocytes (24–26). Therefore, we used flow cytometry to determine the percentages of $CD69^+$ cells

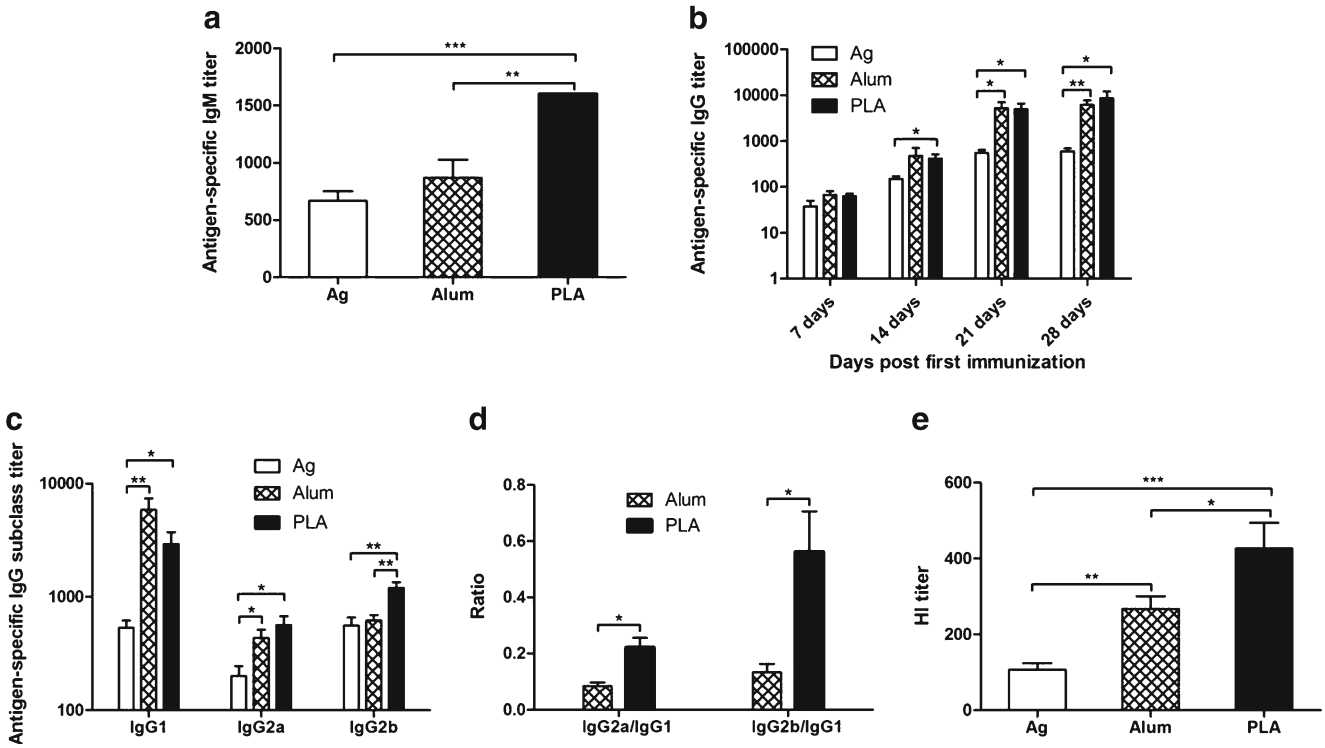

Fig. 2 The effect of PLA microparticles and alum on antigen-specific serum antibody responses. Balb/c mice ($n = 6$) were intramuscularly vaccinated twice at a 2-week interval. ELISA and hemagglutination inhibition (HI) assay were performed to detect antibodies levels in sera collected from immunized mice at the indicated time points. (**a**) Antigen-specific IgM titers in the serum on day 7 after primary immunization. (**b**) Antigen-specific serological IgG titers at different time points post first immunization. (**c**) Antigen-specific IgG1, IgG2a, and IgG2b titers, (**d**) ratios of IgG subclasses, and (**e**) HI titers in serum on day 28 post primary immunization. Data are shown as mean ± SEM ($n = 6$). *$p < 0.05$, **$p < 0.01$, and ***$p < 0.001$.

in B cells, $CD4^+$ T cells and $CD8^+$ T cells in splenocytes harvested from immunized mice. As shown in Fig. 4a and Supplementary Material Fig. S1a–c, the expression of CD69 on B cells, $CD4^+$ T cells and $CD8^+$ T cells was slightly increased by alum, but increased to significantly higher levels by PLA microparticles.

Memory T cells play an important role in controlling secondary infection and eliminating pathogens (27). Effector memory T cells ($CD44^{hi}CD62L^{low}$) recirculate preferentially through non-lymphoid tissue and can immediately respond to re-exposed antigen (28–31). Thus, we next wanted to determine the presence of effector memory T cells after vaccination with different vaccine formulations. Promotion of percentages of effector memory ($CD44^{hi}CD62L^{low}$) cells in $CD4^+$ T cells and $CD8^+$ T cells was achieved by PLA microparticles, but not by alum (Fig. 4b, and Supplementary Material Fig. S1d–e). This result indicated that PLA microparticles were more effective than alum for inducing antigen-specific effector memory T cell response.

To further investigate the effect of both adjuvants on antigen-specific $CD8^+$ T cell response, we analyzed the frequency of antigen-specific $CD8^+$ T cells in spleen using peptide-MHC I pentamer staining, and the degranulation of $CD8^+$ T cells by determining the concentration of granzyme B in culture supernatant of splenocytes re-stimulated *in vitro*. As shown in Fig. 5a–c, no difference was observed in the frequency of antigen-specific $CD8^+$ T cells between mice vaccinated with soluble antigen or alum vaccine. However, the frequency of antigen-specific $CD8^+$ T cells in mice immunized with PLA microparticles-adjuvanted vaccine was significantly higher than those in mice immunized with soluble antigen and alum vaccine ($p < 0.05$). With regard to release of granzyme B, as shown in Fig. 5d, PLA microparticles-based adjuvant significantly increased the release of granzyme B from antigen-specific $CD8^+$ T cells (soluble antigen-particle vaccine, $p < 0.05$). However, the amount of granzyme B secreted by $CD8^+$ T cells from mice immunized with alum vaccine was significantly lower than that for mice vaccinated with soluble antigen ($p < 0.05$). Taken together, the results indicated that PLA microparticles promoted antigen-specific $CD8^+$ T cell response, while alum did not.

Antigen Adjuvanted with PLA Microparticles Drained Away from Injection Sites Whereas Alum vaccine Formed a Depot

We next wanted to analyze mechanisms for the augmented humoral and cellular immunity elicited by both adjuvanted vaccines. To this end, we first evaluated the effect of PLA microparticles and alum on antigen persistence at injection

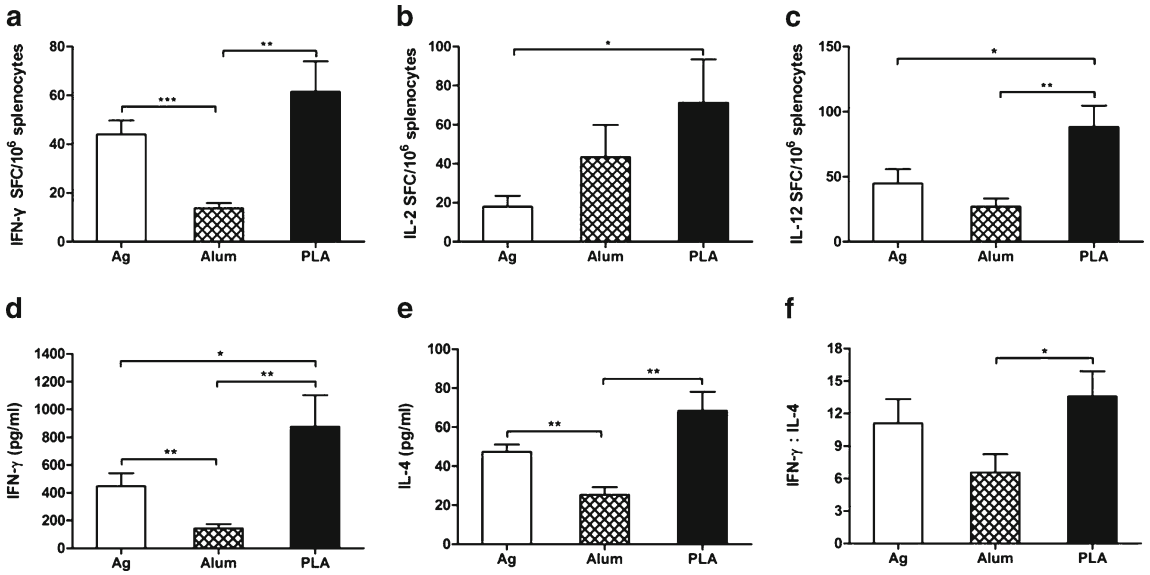

Fig. 3 The effect of PLA microparticles and alum on cytokines secretion by *in vitro* restimulated splenocytes harvested from immunized mice. Balb/c mice ($n = 6$) were intramuscularly vaccinated twice at a 2-week interval. On day 28 post primary immunization, mice were euthanized and splenocytes were harvested. (**a**–**c**) Frequencies of splenocytes secreting (**a**) IFN-γ, (**b**) IL-2, and (**c**) IL-12 were determined by ELISpot assay, according to the manufacturer's instructions. 1.0×10^5 splenocytes in 100 μl medium with H5N1 influenza split vaccine containing 0.25 μg HA as stimulatory agent were added to the wells and the plates were incubated in a 37°C humidified incubator with 5% CO_2 for 36 h. (**d**–**f**) Cytokines level in the culture supernatants of splenocytes. Splenocytes were re-stimulated with HA (cell, 4.0×10^6 cells/ml; HA, 2.0 μg/ml), and cultured for 48 h. The concentration of IFN-γ (**d**) and IL-4 (**e**) were determined using ELISA. The IFN-γ:IL-4 ratio (**f**) was calculated to indicate the Th1/Th2 polarization of vaccine-induced immune response. Data are shown as mean ± SEM ($n = 6$). *$p < 0.05$, **$p < 0.01$, and ***$p < 0.001$.

sites using *in vivo* imaging assay. Various vaccine formulations containing antigen labelled with Cy7 (a near infrared dye) were intramuscularly injected, and fluorescence intensity at injection sites was monitored using an *in vivo* imaging system and quantitatively calculated using Carestream Molecular Imaging Software. The persistence time of antigen adjuvanted by alum was as long as 168 h, but there was no detectable fluorescence at injection site in mice injected with PLA microparticles-adjuvanted vaccine and split vaccine alone, at 4 h and 8 h post injection respectively (Fig. 6a, b). Notably, fluorescence intensity at site injected with PLA microparticles-adjuvanted vaccine decreased more quickly than that for soluble split vaccine injection (Fig. 6b), which was confirmed by more frequent determination of fluorescence intensity attenuation within the first 2 h post injection (Fig. 6c). The results demonstrated that alum and PLA microparticles had opposite effects on antigen persistence at injection sites, *i.e.* alum significantly extending the persistence of antigen at the injection site, but PLA microparticles slightly accelerating the antigen dissemination away from the injection site. The depot effect of alum was based on its positive surface charge and gel characteristic (9). The accelerated antigen drainage away caused by PLA microparticles, might be associated with enhanced antigen uptake by APCs (32), and slightly improved antigen trafficking into draining lymph nodes (no significant difference, Fig. S2 in Supplementary Material).

Alum Induced more Severe Local Inflammation Response than PLA Microparticles

One goal for vaccine development is to reduce local inflammation associated with vaccine injection. Therefore, we next sought to determine the extent of local inflammation induced by different vaccine formulation. Histological examination revealed that alum-adjuvanted vaccine elicited more severe inflammatory response than both soluble split vaccine and PLA microparticles-adjuvanted vaccine on day 2 post injection (Fig. 7, upper panel). 7 days after injection, inflammation caused by soluble split vaccine and PLA microparticles-adjuvanted vaccine disappeared. In contrast, alum-adjuvanted vaccine-induced inflammation became more serious (Fig. 7, lower panel). Thus, unlike PLA microparticles, alum adjuvanted vaccine caused severe inflammation at injection site that persisted for more than 7 days.

Fig. 4 The effect of PLA microparticles and alum on lymphocytes activation and effector memory T cell response. Balb/c mice ($n = 6$) were intramuscularly vaccinated twice at a 2-week interval. On day 28 post primary immunization, mice were euthanized, and splenocytes were harvested and stimulated with HA (HA, 2.5 μg/ml; splenocytes, 5.0×10^6 cells/ml) in a 37°C humidified incubator with 5% CO_2 for 72 h. Flow cytometry assay was performed to determine the percentages of (**a**) activated lymphocytes ($CD69^+$) and (**b**) effector memory ($CD44^{hi}CD62L^{low}$) Tcells. Data are representative for 6 results in each group. ▶

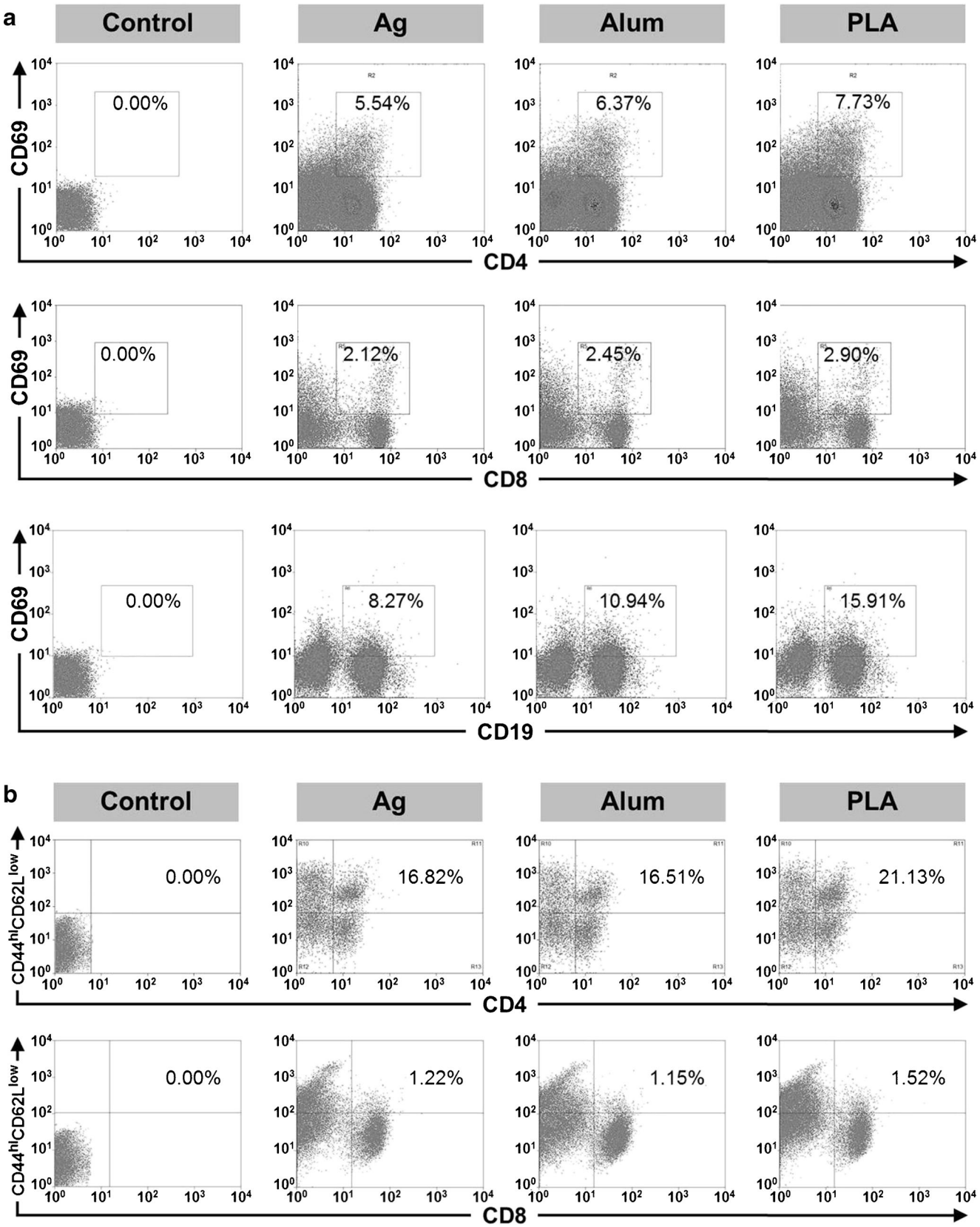
a
Control
Ag
Alum
PLA
CD69
CD4
0.00%
5.54%
6.37%
7.73%
CD8
2.12%
2.45%
2.90%
CD19
8.27%
10.94%
15.91%
b
CD44hiCD62Llow
16.82%
16.51%
21.13%
1.22%
1.15%
1.52%

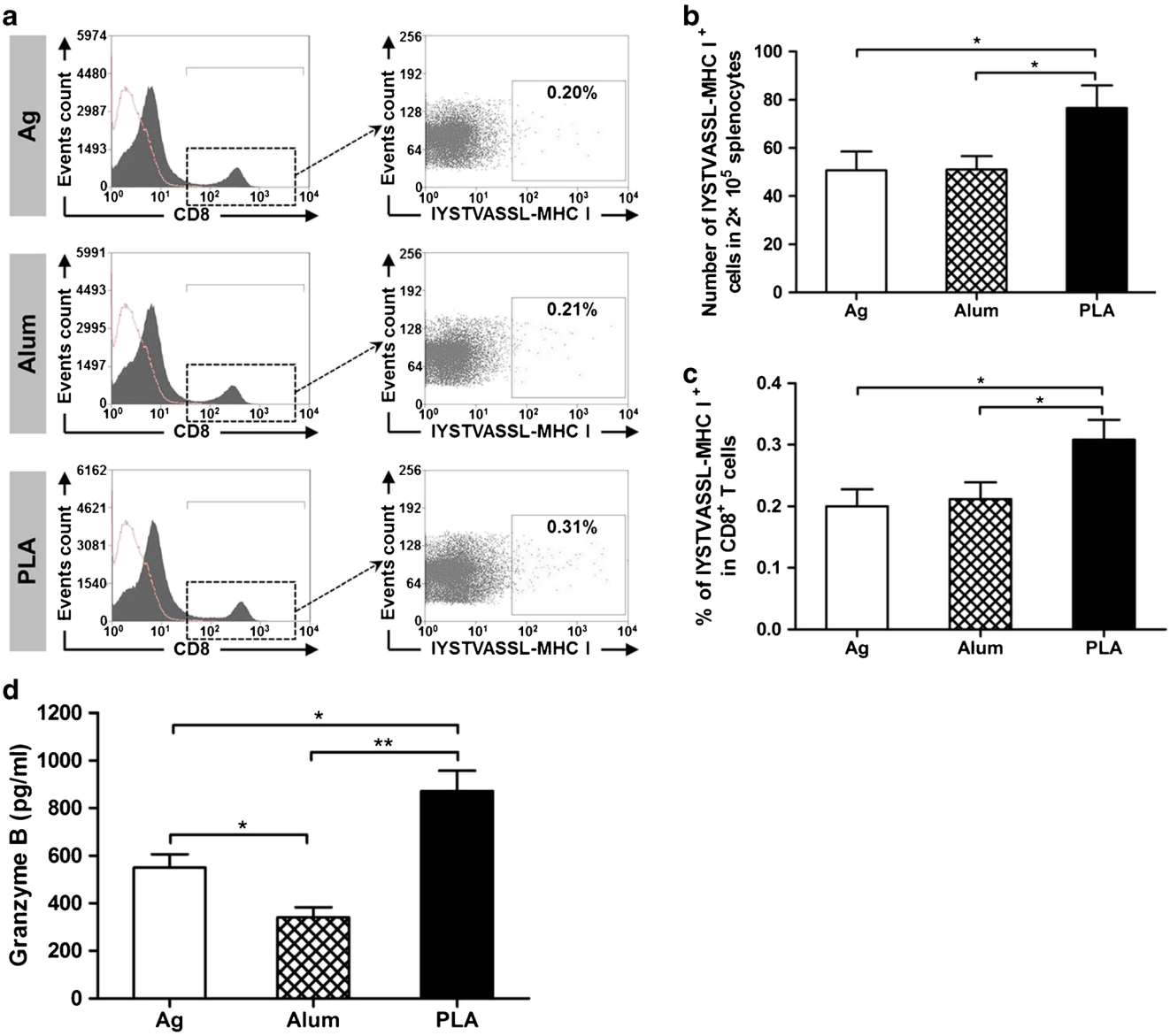

Fig. 5 The effect of PLA microparticles and alum on antigen-specific $CD8^+$ T cell response. Balb/c mice ($n = 6$) were intramuscularly vaccinated twice at a 2-week interval. On day 28 post primary immunization, mice were euthanized, and splenocytes were harvested and re-stimulated with HA (HA, 2.0 μg/ml; splenocytes, 4.0×10^6 cells/ml) in a 37°C humidified incubator with 5% CO_2 for 48 h. Pentamer staining and flow cytometry assay was performed to determine the percentages of IYSTVASSL-MHC I-specific $CD8^+$ T cells. (**a**) Representative flow cytometry plot, (**b**) number of IYSTVASSL-MHC I-specific $CD8^+$ T cells in 2×10^5 splenocytes, and (**c**) percentage of IYSTVASSL-MHC I^+ cells in $CD8^+$ T cells. (**d**) The amount of granzyme B in the supernatant was measured by ELISA. Data are shown as mean ± SEM ($n = 6$). *$p < 0.05$, **$p < 0.01$, and ***$p < 0.001$.

Effect of both Adjuvants on Maturation and Activation of DCs in Secondary Lymphoid Organs

Maturation of antigen presenting cell is a prerequisite of antigen presentation and subsequent T cells activation (33). MHC molecules are important surface markers indicating the maturation level of APCs and potential pathways of subsequent antigen presentation (34). Therefore, we next determined the expression of MHC I and MHC II on dendritic cells in secondary lymphoid organs by flow cytometry. Compared to soluble split vaccine, both alum- and PLA microparticles-adjuvanted vaccines didn't remarkably improve the expression level of MHC I and MHC II on dendritic cells in sciatic and popliteal lymph nodes 2 days and 7 days after immunization (data not shown). However, alum significantly enhanced the expression of MHC II on splenic DCs at 7 days after immunization (Fig. 8a and c), and PLA microparticles augmented the expression of both MHC I and MHC II on splenic DCs on day 7 post immunization (Fig. 8a–c). The higher level of MHC I molecule expressed on DCs induced by PLA microparticles-adjuvanted vaccine suggests a stronger MHC I-restricted pathway, which is favorable for cell-mediated immunity.

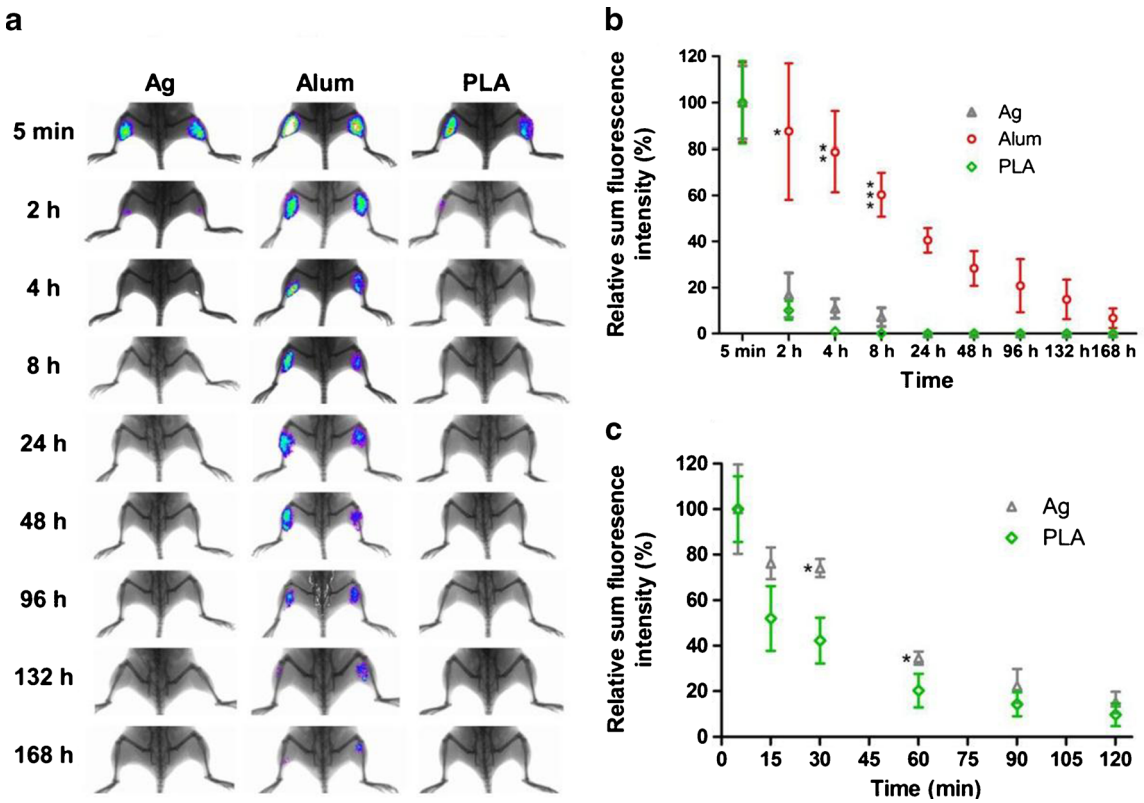

Fig. 6 Antigen persistence at injection sites. Balb/c mice ($n = 6$) were intramuscularly injected with different vaccine formulations containing Ag-Cy7. The retention of antigen at injection sites was documented by *in vivo* imaging system at the indicated time points. Carestream Molecular Imaging Software was used to quantify the sum fluorescence intensity at the injection sites. (**a**) Representative fluorescent images and (**b**) quantitative fluorescence intensity of antigen retaining at injection sites from 5 min to 168 h post injection. (**c**) Quantitative fluorescence intensity of antigen retaining at injection sites in the first 2 h post injection (split vaccine and PLA microparticles-adjuvanted vaccine). Data in (**a**) are representative for 6 results in each group. $^{*}p < 0.05$, $^{**}p < 0.01$, and $^{***}p < 0.001$.

Fig. 7 Histological evaluation of vaccine-associated inflammation at injection sites. Balb/c mice ($n = 3$) were intramuscularly injected with different vaccine formulations. At 2 and 7 days post injection, muscles tissue from injection sites were isolated from mice, embedded in paraffin, sectioned, and stained with hematoxylin and eosin to evaluate inflammation. Data are representative for 6 results in each group. Arrows indicate areas with inflammation.

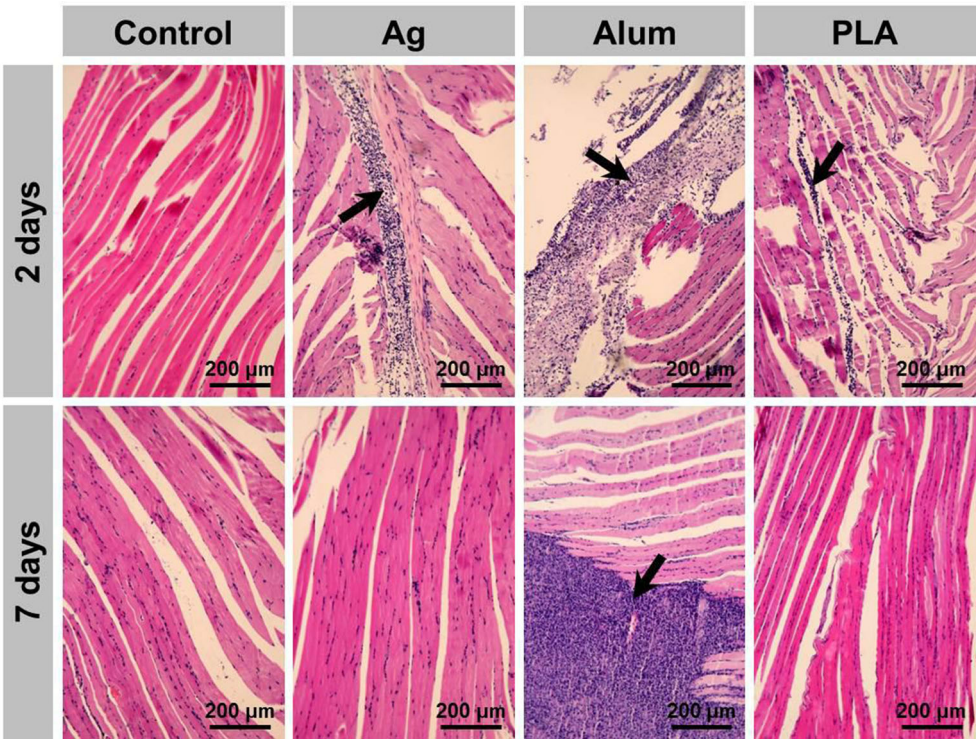

With regard to co-stimulatory molecules (CD80 and CD86) expression on DCs, no difference was observed in CD80 expression on DCs in draining lymph nodes for all vaccine formulation (data not shown). As shown in Fig. 9a and b, PLA microparticles increased the expression of CD86 molecule on DCs in draining lymph node (24 h, PLA microparticles-adjuvanted vaccine *vs* soluble antigen: $p < 0.05$). However, compared to soluble antigen, alum significantly reduced the expression of CD86 molecule (alum vaccine *vs* soluble antigen: 12 h, $p < 0.05$; 24 h, 2 days, $p < 0.01$). On the whole, PLA microparticles improved the expression of co-stimulatory molecules on DCs in draining lymph node, while alum depressed the expression.

DISCUSSION

Vaccines play important roles in protecting individuals against pathogens and controlling infections. Considering safety concerns, subunit vaccines (split vaccine or purified protein) have evident advantages over pathogen-based vaccine (attenuated or inactivated virus). However, owing to the low immunogenicity of subunit vaccine, adjuvants have to be included to augment the immune response. In this study, we compared the adjuvanticity of PLA microparticles and alum for H5N1 influenza split vaccine, especially their potential to augment cell mediated immunity, and investigated respective mode of action.

When polymeric particles were used as adjuvant, antigen could be encapsulated into particles, adsorbed on the particle surface, conjugated onto the particle surface, or simply mixed with particles. In this study, considering antigen-saving and the convenience for practical application, we choosed mixture-adsorption method to prepare PLA microparticles adjuvanted vaccine formulation. Because encapsulation method or conjugation method is more complicated and time-consuming, and will result in incomplete utilization of antigen. It's impracticable for influenza vaccine, because large quantity of vaccine is urgently needed when pandemics appears. Formulating antigen with adjuvant by adsorbing or mixing, is convenient for rapid vaccine production and beneficial to antigen-saving. Facilitating antigen uptake by antigen presenting cells (APCs) is one of the mechanisms of action of particles adjuvant. We believe that antigen adsorption to the microparticles is beneficial for antigen uptake by APCs. Not removing unbound antigens is based on the consideration of antigen saving.

IgM accounts for 5–10% of the total serum immunoglobulin, and is the first immunoglobulin class produced in a primary response to an antigen. IgM plays important roles in binding antigens with many repeating epitopes, agglutinating, neutralizing viral infectivity, and activating complement system (35,36). Thus, IgM antibody level is an indicator of early humoral response. PLA microparticles-adjuvanted vaccine induced higher serum IgM titers than alum-based vaccine (Fig. 2a). These data suggest PLA microparticles as adjuvant induced stronger immune response at the early stage after vaccination.

IgG, on the other hand, is the main antibody class in blood and extracellular fluid, and plays a key role in controlling infection. Although IgG titer increased to comparable levels by employment of alum or PLA microparticles as adjuvant, IgG subclasses profile suggested that immunization with PLA microparticles-adjuvanted vaccine elicited IgG2a- and IgG2b-dominated antibody response and vaccination with alum-adjuvanted vaccine induced IgG1-dominated antibody response (Fig. 2b–d). IgG is consisted of four structurally and functionally distinct subclasses in humans and mice. IgG1, IgG2a, and IgG2b are main subclasses elicited by protein antigens. All IgG subclasses recognize antigen on foreign cells, but have specialized effector responses and significantly different abilities to eliminate these foreign targets. Because different IgG subclasses have differential affinity for activatory and inhibitory Fcγ receptors (FcγRs) frequently co-expressed on immune cells, such as macrophages and monocytes. The affinity for activatory and inhibitory FcγRs is defined as activatory-to-inhibitory (A/I) ratio. A/I ratios of IgG1, IgG2a, and IgG2b are 0.1, 69, and 7, respectively (37,38). Therefore, IgG2a and IgG2b are the most potent for activating effector responses, and ratios of IgG2a/IgG1 and IgG2b/IgG1 can be recognized as indicators of Th1/Th2 polarization (39–41). Therefore, PLA microparticles exerted more significant effect on cellular immunity than alum. The effect of both adjuvants on augmentation of cellular immunity was confirmed by determination of Th1 cytokines secreted by splenocytes restimulated *in vitro*, because Th1 cytokines could directly promote cell-mediated-immunity (23). The improved cell-mediated immunity might more efficiently protected against infection of influenza virus with high variability. According to the results above, alum just increased the quantity of immune response, but PLA microparticles improved both the quantity and the quality of immune response.

Alum is the mostly used adjuvant for human vaccine, and its adjuvanticity is associated with enhanced antibody response, contributing little to, or even suppressing, cell-mediated immunity (9,42–45). Reportedly, alum acts by forming antigen depot to achieve gradual release of antigen (45,46), and inducing local inflammation to recruit neutrophils and monocytes (47). Our study confirmed these reports, through the *in vivo* imaging study

Fig. 8 The effect of PLA microparticles and alum on maturation of splenic DCs. Balb/c mice ($n = 3$) were intramuscularly vaccinated with different vaccine formulations. At the time points of 2 days and 7 days post immunization, mice were euthanized and splenocytes were isolated. Expression of MHC molecules on dendritic cells was determined by flow cytometry. (**a**) Representative flow cytometry plot (7 days); (**b**) Relative fluorescence intensity of MHC I expressed on DCs; and (**c**) Relative fluorescence intensity of MHC II molecule expressed on DCs. Data are shown as mean ± SEM ($n = 3$). *$p < 0.05$.

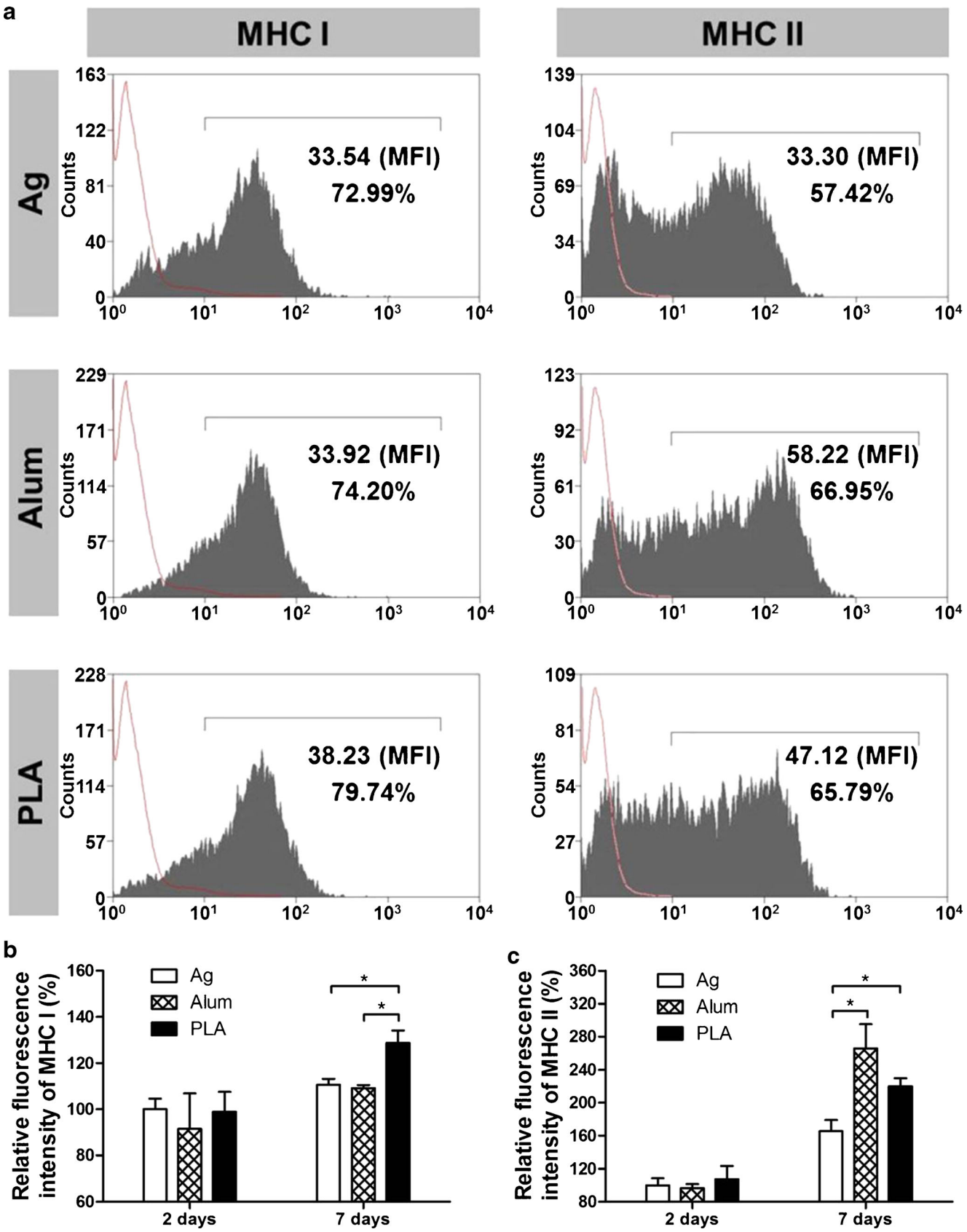
a
MHC I
MHC II
Ag
Alum
PLA
Counts
33.54 (MFI)
72.99%
33.30 (MFI)
57.42%
33.92 (MFI)
74.20%
58.22 (MFI)
66.95%
38.23 (MFI)
79.74%
47.12 (MFI)
65.79%
b
Relative fluorescence intensity of MHC I (%)
Ag
Alum
PLA
2 days
7 days
c
Relative fluorescence intensity of MHC II (%)
Ag
Alum
PLA
2 days
7 days

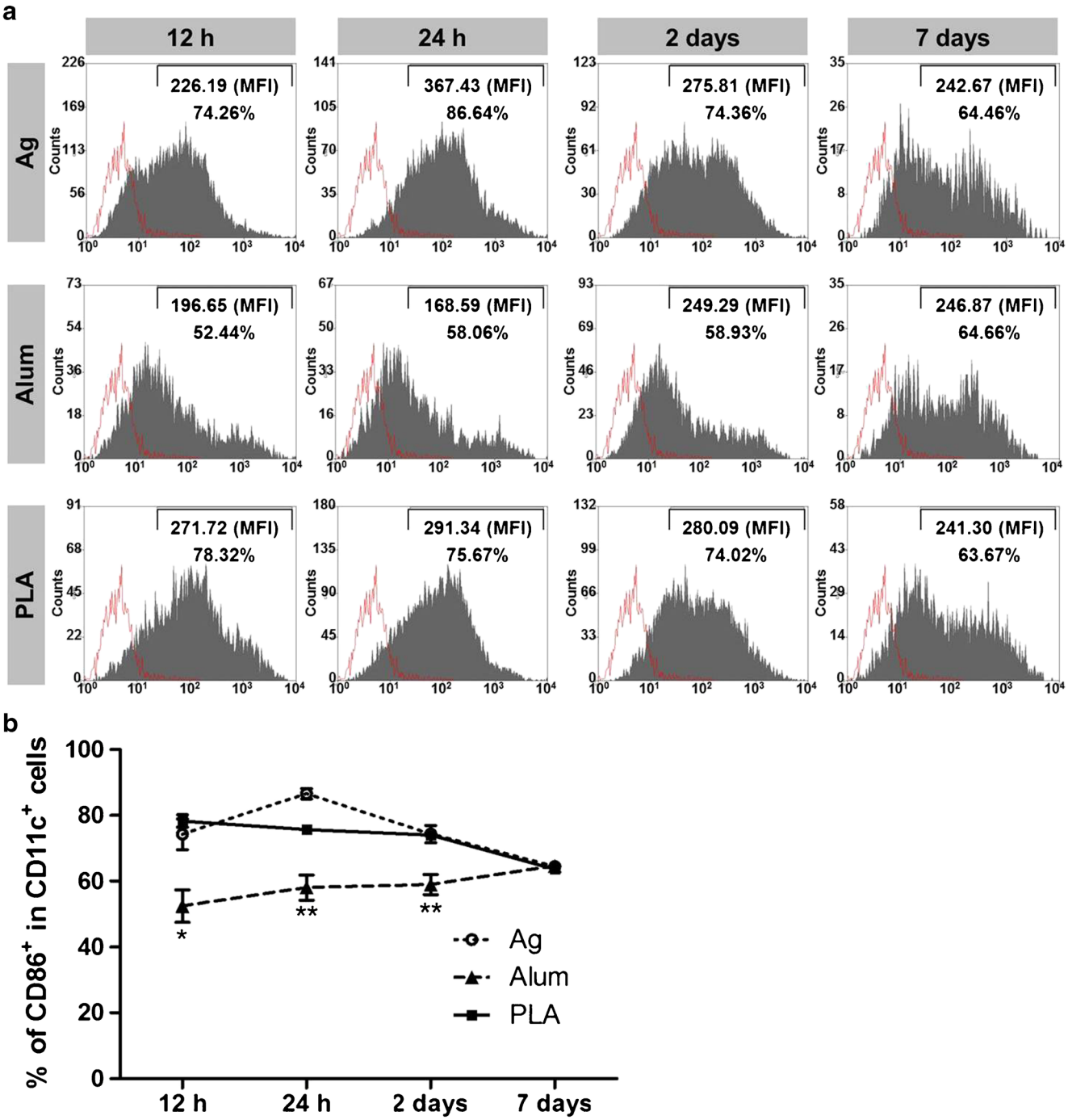

Fig. 9 The effect of PLA microparticles and alum on activation of dendritic cells in spleen. Balb/c mice ($n = 4$) were intramuscularly vaccinated with different vaccine formulations. At the indicated time points post immunization, mice were euthanized and single cell suspension was prepared from draining lymph nodes (popliteal lymph nodes). The cells were stained with anti-CD11c antibody and anti-CD86 antibody (eBioscience, USA). Expression of co-stimulatory molecule CD86 on dendritic cells was determined by flow cytometry. (**a**) Representative flow cytometry plot; (**b**) Percentage of $CD86^+$ cells in $CD11c^+$ DCs at different time points post vaccine injection. Data are shown as mean ± SEM ($n = 4$). *$p < 0.05$, **$p < 0.01$.

of antigen persistence at injection sites (Fig. 6a–b) and histological evaluation of local inflammatory response (Fig. 7). In addition, the previously reported effects of alum (9,42–45), were also observed in this study, including a poor induction of IgG2a and IgG2b antibodies, Th1 cytokines, and antigen-specific $CD8^+$ T cell response. This effect might be attributed to sequestration of antigen at the injection site and consequent low antigen availability in secondary lymphoid organs. This is consistent with previous studies demonstrating that IgG1 and Th2 cytokines were response to very low antigen doses, while production of IgG2a antibody and Th1 cytokines required higher antigen doses (48).

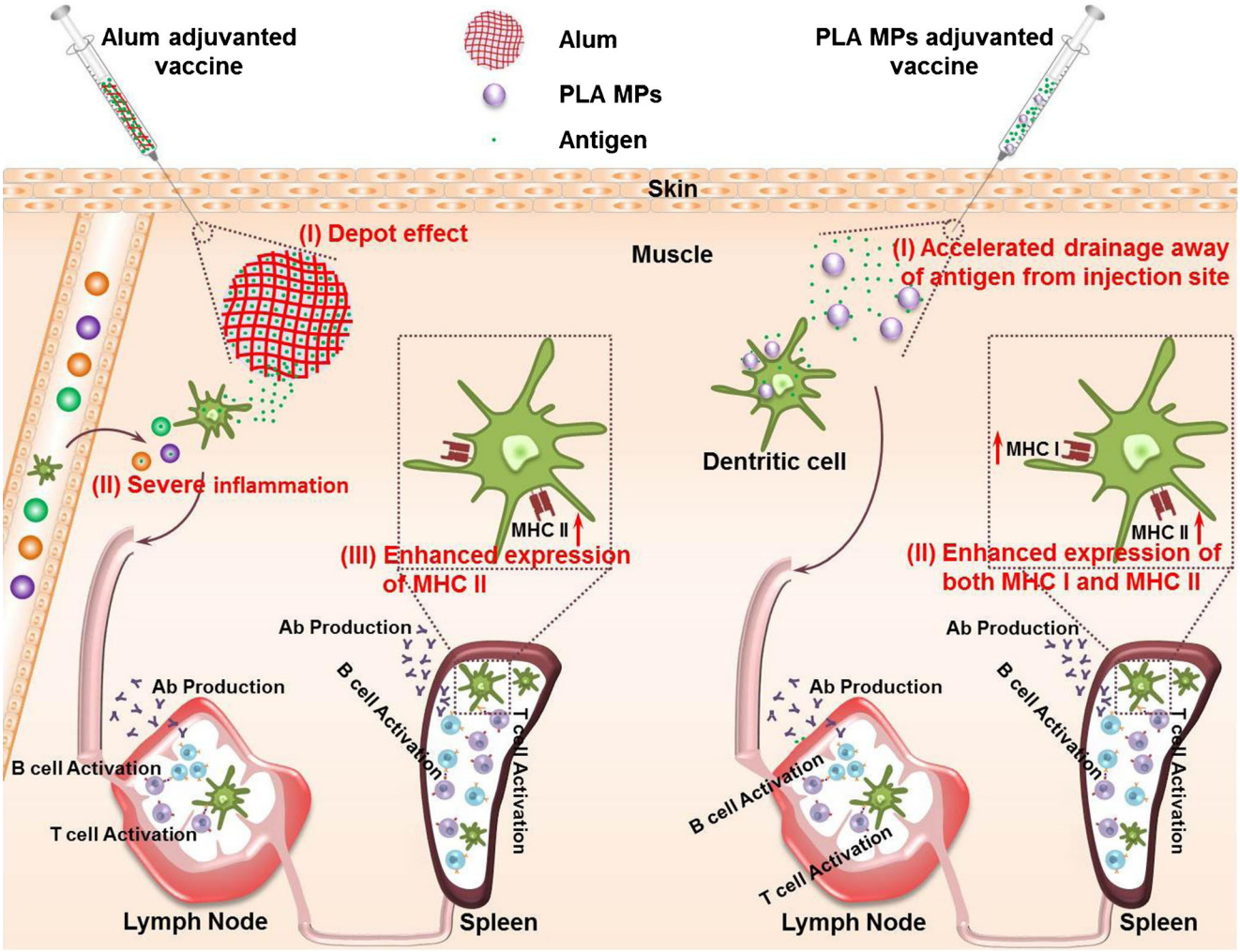

Fig. 10 Schematic illustration of action modes of PLA microparticles and alum. Alum significantly enhanced antigen persistence at injection sites, induced severe local inflammation response, and improved the expression of MHC II on splenic DCs; However, it induced severe local inflammatory response. Alternatively, PLA microparticles slightly enhanced the drainage away of antigen from injection sites, induced mild local inflammation response, favored antigen transport into draining lymph nodes, and promoted the expression of both MHC molecules and co-stimulatory molecule on DCs in secondary lymphoid organs, inducing mild local inflammation.

Biodegradable particulate delivery system, as a kind of new generation adjuvant, holds great promise for the development of novel vaccines, especially cellular vaccines. In the present study, determination of IgG subclasses profile (Fig. 2c, d), cytokines secretion by splenocytes (Fig. 3), effector memory T cell response (Fig. 4b), and antigen-specific $CD8^+$ T cell response (Fig. 5a–c) suggested that PLA microparticles could augment not only humoral immune response, but also cell-mediated-immunity which might enhance the cross-protection of H5N1 influenza vaccine. The adjuvant effect of PLA microparticles might be attributed to improving antigen uptake by APCs, adjusting antigen presentation pathways (as described in our previous work (32)), and slightly promoting antigen trafficking to draining lymph nodes (no significant difference, Fig. S2 in Supplementary Material). Because comparable dimensions to pathogens favor the uptake of particulates by antigen presenting cells (14,45). And the effect of polymeric particulates on endo-lysosomal escape, and cross-presentation of exogenous antigen had been defined by many researchers (34,45,49–51). What's more, promoting antigen transport into draining lymph nodes might be one of the mechanisms by which PLA microparticles augmented cell-mediated immunity. Because production of IgG2a antibody and Th1 cytokines required higher antigen doses (48).

Toxicity and safety concerns are crucial issues in adjuvant development, and the potency of adjuvants has to be strictly balanced with their potential adverse side effects. Despite of its wide use for over 80 years, alum did have caused some side effects and safety problems, including IgE-associated allergic reaction (45), macrophagic myofasciitis, the potential for cumulative alum toxicity which has been associated with amyotrophic lateral sclerosis, Alzheimer's disease and dialysis-associated dementia (16). As a potent alternative, PLA is biodegradable, biocompatible, non-toxic, non-immunogenic,

FDA-approved polymer and easily processed into particles (14,52). Moreover, PLA-based particulates have been widely used as medical devices and drug/vaccine delivery systems for many years with a strong safety record (14,33,45). In this study, results of histological examination of sectioned muscle containing injection site, *i.e.* that alum elicited significantly severe local inflammatory response than PLA microparticles (Fig. 7), were in accordance with previous reports (53). Therefore, these data suggest that PLA microparticles are not only a kind of more potent adjuvant, but also exerted much milder adverse side effect than alum.

Based on the result of this study, we propose the following model (Fig. 10). Alum may enhance the immunogenicity of split vaccine by (I) significantly improving antigen persistence at injection sites (*i.e.* antigen depot effect) to achieve sustained release of antigen, (II) inducing severe local inflammation which recruited a large number of immune cells (such as neutrophils, monocytes, eosinophils, dendritic cells, and macrophages) to injection sites (47), and (III) promoting the expression of MHC II molecule on splenic DCs. However, PLA microparticles (I) slightly accelerated antigen dissemination away from injection sites, (II) slightly favored antigen transport into draining lymph nodes, and significantly promoted the expression of both MHC molecules (MHC I and MHC II) and co-stimulatory molecules on DCs in secondary lymphoid organs, which might be beneficial to simultaneous augmentation of humoral and cell mediated immunity.

CONCLUSIONS

In conclusion, this study reveals that PLA microparticles and alum exerted their adjuvant activities through different modes of action, had different adjuvanticity for H5N1 influenza split vaccine, and induced different levels of adverse side effects. Alum- and PLA microparticles-adjuvanted vaccines induced comparable serum IgG titer, while PLA microparticles-adjuvanted vaccine elicited higher level of IgM response in the early stage and higher HI titers. Moreover, PLA microparticles induced stronger Th1 polarization and antigen-specific $CD8^+$ T cell response, which might contribute to the cross-protection of influenza vaccine. With respect to action mode, both adjuvants slightly promote antigen transport into draining lymph nodes. Alum significantly enhanced antigen persistence at injection sites, and improved the expression of MHC II on splenic DCs. On the contrary, PLA microparticles slightly enhanced the dissemination away of antigen from injection sites, and improved the expression of both MHC molecules and co-stimulatory molecules on dendritic cells. Alum induced severe local inflammation, while PLA microparticles din not. Considering the efficacy and side effect of both adjuvants, we conclude that PLA microparticles are promising alternative adjuvant for H5N1 influenza split vaccine.

ACKNOWLEDGMENTS AND DISCLOSURES

The authors gratefully thank Dr Wei Wei for assistance with CLSM characterization of PLA microparticles-adjuvanted vaccine formulation. This work was financially supported by the 973 Program (Grant No. 2013CB531500), the Knowledge Innovation Program of the Chinese Academy of Sciences (Grant No. KSCX2-EW-R-19), and the 863 Program (Grant No. 2012AA02A406).

REFERENCES

1. Subbarao K, Joseph T. Scientific barriers to developing vaccines against avian influenza viruses. Nat Rev Immunol. 2007;7(4):267–78.
2. Horimoto T, Kawaoka Y. Strategies for developing vaccines against H5N1 influenza A viruses. Trends Mol Med. 2006;12(11):506–14.
3. Geeraedts F, Goutagny N, Hornung V, Severa M, de Haan A, Pool J, *et al*. Superior immunogenicity of inactivated whole virus H5N1 influenza vaccine is primarily controlled by toll-like receptor signalling. PLoS Pathog. 2008;4(8):e1000138.
4. Stropkovska A, Janulikova J, Vareckova E. Trends in development of the influenza vaccine with broader cross-protection. Acta Virol. 2010;54(1):7–19.
5. Brown LE, Kelso A. Prospects for an influenza vaccine that induces cross-protective cytotoxic T lymphocytes. Immunol Cell Biol. 2009;87(4):300–8.
6. Carrat F, Flahault A. Influenza vaccine: the challenge of antigenic drift. Vaccine. 2007;25(39–40):6852–62.
7. Tamura SI, Tanimoto T, Kurata T. Mechanisms of broad cross-protection provided by influenza virus infection and their application to vaccines. Jpn J Infect Dis. 2005;58(4):195–207.
8. Doherty PC, Kelso A. Toward a broadly protective influenza vaccine. J Clin Invest. 2008;118(10):3273–5.
9. Marrack P, McKee AS, Munks MW. Towards an understanding of the adjuvant action of aluminium. Nat Rev Immunol. 2009;9(4):287–93.
10. Mbow ML, De Gregorio E, Valiante NM, Rappuoli R. New adjuvants for human vaccines. Curr Opin Immunol. 2010;22(3):411–6.
11. Exley C, Siesjö P, Eriksson H. The immunobiology of aluminium adjuvants: how do they really work? Trends Immunol. 2010;31(3):103–9.
12. Sharp FA, Ruane D, Claass B, Creagh E, Harris J, Malyala P, *et al*. Uptake of particulate vaccine adjuvants by dendritic cells activates the NALP3 inflammasome. Proc Natl Acad Sci U S A. 2009;106(3):870–5.
13. Harris J, Sharp FA, Lavelle EC. The role of inflammasomes in the immunostimulatory effects of particulate vaccine adjuvants. Eur J Immunol. 2010;40(3):634–8.
14. Broaders KE, Cohen JA, Beaudette TT, Bachelder EM, Fréchet JMJ. Acetalated dextran is a chemically and biologically tunable material for particulate immunotherapy. Proc Natl Acad Sci U S A. 2009;106(14):5497–502.
15. Yanasarn N, Sloat BR, Cui Z. Negatively charged liposomes show potent adjuvant activity when simply admixed with protein antigens. Mol Pharm. 2011;8(4):11741185.
16. Zaharoff DA, Rogers CJ, Hance KW, Schlom J, Greiner JW. Chitosan solution enhances both humoral and cell-mediated immune responses to subcutaneous vaccination. Vaccine. 2007;25(11):2085–94.
17. Wei Q, Wei W, Lai B, Wang L-Y, Wang Y-x, Su Z-G, *et al*. Uniform-sized PLA nanoparticles: preparation by premix membrane emulsification. Int J Pharm. 2008;359(1–2):294–7.
18. Amidi M, Romeijn SG, Verhoef JC, Junginger HE, Bungener L, Huckriede A, *et al*. N-Trimethyl chitosan (TMC) nanoparticles

loaded with influenza subunit antigen for intranasal vaccination: biological properties and immunogenicity in a mouse model. Vaccine. 2007;25(1):144–53.
19. Bright RA, Carter DM, Crevar CJ, Toapanta FR, Steckbeck JD, Cole KS, *et al*. Cross-clade protective immune responses to influenza viruses with H5N1 HA and NA elicited by an influenza virus-like particle. PLoS One. 2008;3(1):e1501.
20. Hagenaars N, Mastrobattista E, Verheul R, Mooren I, Glansbeek H, Heldens J, *et al*. Physicochemical and immunological characterization of N, N, N-Trimethyl Chitosan-coated whole inactivated influenza virus vaccine for intranasal administration. Pharmaceut Res. 2009;26(6):1353–64.
21. Chesko J, Kazzaz J, Ugozzoli M, O'Hagan DT, Singh M. An investigation of the factors controlling the adsorption of protein antigens to anionic PLG microparticles. J Pharm Sci. 2005;94(11):2510–9.
22. Horimoto T, Kawaoka Y. Influenza: lessons from past pandemics, warnings from current incidents. Nat Rev Micro. 2005;3(8):591–600.
23. Ma Y, Zhuang Y, Xie X, Wang C, Wang F, Zhou D, *et al*. The role of surface charge density in cationic liposome-promoted dendritic cell maturation and vaccine-induced immune responses. Nanoscale. 2011;3(5):2307–14.
24. Marzio R, Mauël J, Betz-Corradin S. CD69 and regulation of the immune function. Immunopharm Immunot. 1999;21(3):565–82.
25. Nygaard UC, Ormstad H, Aase A, Løvik M. The IgE adjuvant effect of particles: characterisation of the primary cellular response in the draining lymph node. Toxicology. 2005;206(2):181–93.
26. Lindsey W, Lowdell M, Marti G, Abbasi F, Zenger V, King K, *et al*. CD69 expression as an index of T-cell function: assay standardization, validation and use in monitoring immune recovery. Cytotherapy. 2007;9(2):123–32.
27. Kaech SM, Wherry EJ, Ahmed R. Effector and memory T-cell differentiation: implications for vaccine development. Nat Rev Immunol. 2002;2(4):251–62.
28. Wherry EJ, Teichgraber V, Becker TC, Masopust D, Kaech SM, Antia R, *et al*. Lineage relationship and protective immunity of memory CD8 T cell subsets. Nat Immunol. 2003;4(3):225–34.
29. Thakur A, Pedersen LE, Jungersen G. Immune markers and correlates of protection for vaccine induced immune responses. Vaccine. 2012;30(33):4907–20.
30. Patel A, Zhang Y, Croyle M, Tran K, Gray M, Strong J, *et al*. Mucosal delivery of adenovirus-based vaccine protects against ebola virus infection in mice. J Infect Dis. 2007;196(2):S413–20.
31. Trimnell A, Takagi A, Gupta M, Richie TL, Kappe SH, Wang R. Genetically attenuated parasite vaccines induce contact-dependent CD8+ T cell killing of plasmodium yoelii liver stage-infected hepatocytes. J Immunol. 2009;183(9):5870–8.
32. Yue H, Wei W, Fan B, Yue Z, Wang L, Ma G, *et al*. The orchestration of cellular and humoral responses is facilitated by divergent intracellular antigen trafficking in nanoparticle-based therapeutic vaccine. Pharmacol Res. 2012;65(2):189–97.
33. Singh M, Chakrapani A, O'Hagan D. Nanoparticles and microparticles as vaccine-delivery systems. Expert Rev Vaccines. 2007;6(5):797–808.
34. Han RL, Zhu JM, Yang XL, Xu HB. Surface modification of poly(D, L-lactic-co-glycolic acid) nanoparticles with protamine enhanced cross-presentation of encapsulated ovalbumin by bone marrow-derived dendritic cells. J Biomed Mater Res Part A. 2011;96A(1):142–9.
35. Klimovich V. IgM and its receptors: structural and functional aspects. Biochem Mosc. 2011;76(5):534–49.
36. Saini V, Jain V, Sudheesh MS, Jaganathan KS, Murthy PK, Kohli DV. Comparison of humoral and cell-mediated immune responses to cationic PLGA microspheres containing recombinant hepatitis B antigen. Int J Pharm. 2011;408(1–2):50–7.
37. Nimmerjahn F, Ravetch JV. Divergent immunoglobulin G subclass activity through selective Fc receptor binding. Science. 2005;310(5753):1510–2.
38. Woof JM. Tipping the scales toward more effective antibodies. Science. 2005;310(5753):1442–3.
39. Zhang S, Cubas R, Li M, Chen C, Yao Q. Virus-like particle vaccine activates conventional B2 cells and promotes B cell differentiation to IgG2a producing plasma cells. Mol Immunol. 2009;46(10):1988–2001.
40. Nimmerjahn F, Ravetch JV. Fcγ receptors: old friends and new family members. Immunity. 2006;24(1):19–28.
41. Bian G, Cheng Y, Wang Z, Hu Y, Zhang X, Wu M, *et al*. Whole recombinant Hansenula polymorpha expressing hepatitis B virus surface antigen (yeast-HBsAg) induces potent HBsAg-specific Th1 and Th2 immune responses. Vaccine. 2009;28(1):187–94.
42. Kanchan V, Panda AK. Interactions of antigen-loaded polylactide particles with macrophages and their correlation with the immune response. Biomaterials. 2007;28(35):5344–57.
43. Chen X, Kim P, Farinelli B, Doukas A, Yun S-H, Gelfand JA, *et al*. A novel laser vaccine adjuvant increases the motility of antigen presenting cells. PLoS One. 2010;5(10):e13776.
44. Singh M, O'Hagan DT. Recent advances in vaccine adjuvants. Pharmaceut Res. 2002;19(6):715–28.
45. Hagan DT, Singh M. Microparticles as vaccine adjuvants and delivery systems. Expert Rev Vaccines. 2003;2(2):269–83.
46. Tritto E, Mosca F, De Gregorio E. Mechanism of action of licensed vaccine adjuvants. Vaccine. 2009;27(25–26):3331–4.
47. Calabro S, Tortoli M, Baudner BC, Pacitto A, Cortese M, O'Hagan DT, *et al*. Vaccine adjuvants alum and MF59 induce rapid recruitment of neutrophils and monocytes that participate in antigen transport to draining lymph nodes. Vaccine. 2011;29(9):1812–23.
48. Mohanan D, Slütter B, Henriksen-Lacey M, Jiskoot W, Bouwstra JA, Perrie Y, *et al*. Administration routes affect the quality of immune responses: a cross-sectional evaluation of particulate antigen-delivery systems. J Control Release. 2010;147(3):342–9.
49. Shen H, Ackerman AL, Cody V, Giodini A, Hinson ER, Cresswell P, *et al*. Enhanced and prolonged cross-presentation following endosomal escape of exogenous antigens encapsulated in biodegradable nanoparticles. Immunology. 2006;117(1):78–88.
50. PANYAM J, W-Z ZHOU, PRABHA S, SAHOO SK, LABHASETWAR V. Rapid endo-lysosomal escape of poly(dl-lactide-co-glycolide) nanoparticles: implications for drug and gene delivery. FASEB J. 2002;16(10):1217–26.
51. De Koker S, Lambrecht BN, Willart MA, van Kooyk Y, Grooten J, Vervaet C, *et al*. Designing polymeric particles for antigen delivery. Chem Soc Rev. 2011;40(1):320–39.
52. Zhou S, Liao X, Li X, Deng X, Li H. Poly-d, l-lactide–co-poly(ethylene glycol) microspheres as potential vaccine delivery systems. J Control Release. 2003;86(2–3):195–205.
53. Huntimer L, Ramer-Tait AE, Petersen LK, Ross KA, Walz KA, Wang C, *et al*. Evaluation of biocompatibility and administration site reactogenicity of polyanhydride-particle-based platform for vaccine delivery. Adv Healthc Mater. 2013;2(2):369–78.